



PARIS 2017

Th A3 03

Addressing Viscous Effects in Acoustic Full-waveform Inversion

O. Calderon Agudo* (Imperial College London), N. Vieira da Silva (Imperial College London), M. Warner (Imperial College London), J. Morgan (Imperial College London)

Summary

Seismic waves are attenuated and dispersed as they travel through the subsurface given that part of the energy is lost into heat. These effects are visible on the recorded seismic data but are commonly ignored when performing acoustic full-waveform inversion (FWI). As a result, the recovered P-wave velocity models are not as well resolved and are quantitatively less accurate. Here we analyse the impact of viscous effects in acoustic FWI of visco-acoustic synthetic data and we propose and apply a method to mitigate attenuation effects while still performing acoustic FWI, which is based on matching filters. We show that only a smooth model of attenuation is required to successfully improve the recovered P-wave velocity model, even when applied to a noisy synthetic dataset.

Introduction

The physical properties of the earth cause the seismic waves propagating through the subsurface to attenuate and disperse. Typically, these effects are not fully accounted for when inverting large datasets and the 3D acoustic anisotropic wave equation is used in FWI to obtain good quality P-wave velocity models of the subsurface. Attenuation effects are visible in the recorded data and affect all frequencies, including the low frequencies commonly used in FWI (Stopin et al., 2016). Figure 1 shows the phase dispersion and amplitude decrease introduced by attenuation when modelling wave propagation in a simple homogeneous medium. Performing acoustic FWI on such data would lead to inaccuracies in the recovered velocity model, with velocities that are too slow due to the phase delay and amplitude decrease introduced by attenuation. Thus, accounting for these effects should lead to better resolved and more accurate quantitative P-wave velocity models (Warner et al., 2012).

Local inversion strategies have been used to successfully invert for P-wave velocity and attenuation and mitigate the cross-talk of different inversion parameters in visco-acoustic FWI (e.g. Kamei and Pratt, 2013). Here we adapt a method suggested by Agudo et al. (2016) that was originally designed to account for elastic effects, to mitigate attenuation effects in acoustic FWI of visco-acoustic data. Firstly, we study the impact of attenuation in the recovered P-wave velocity models when applying an acoustic inversion to visco-acoustic synthetic data. We then demonstrate that our proposed workflow leads to an improved P-wave velocity model in the presence of attenuation effects while still performing acoustic FWI.

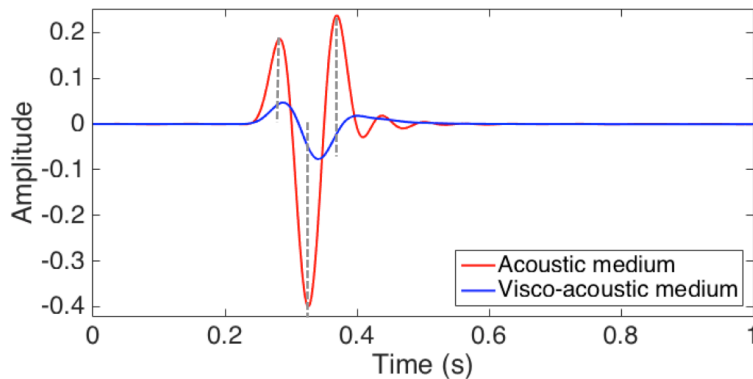


Figure 1 Recorded pressure signal in a homogeneous medium with a P-wave velocity of 2000 m/s without attenuation (red line) and with attenuation (blue line, quality factor $Q=30$).

Methodology

We adapt the workflow proposed by Agudo et al. (2016) to address viscous effects introduced by performing an acoustic inversion of visco-acoustic data. The workflow used is as follows:

1. Acoustic inversion of visco-acoustic data.
2. Generation of synthetic acoustic and visco-acoustic data using the recovered P-wave velocity model and an estimate of the Q model.
3. Computation of matching filters that match the modelled visco-acoustic to the modelled acoustic data obtained in Step 2.
4. Application of the matching filters to the observed data to mitigate viscous effects.
5. Smoothing of the P-wave velocity model recovered in Step 1.
6. Acoustic inversion of the matched observed data obtained in Step 4 using the smoothed model from Step 5 as a starting model.

Step 5 was added as it was found to accelerate the improvements introduced by the matching filters when mitigating visco-acoustic effects, especially if the workflow is applied iteratively by re-starting from Step 2. Repetition of the workflow leads to an improved result but it also increases the computation time, as it requires two additional forward modelling steps and an extra acoustic inversion per iteration.

Results: Marmousi2 model

We now test the proposed method to mitigate visco-acoustic effects on the marine Marmousi2 model (Figure 2a). We design an attenuation model (Figure 2b) that smoothly increases with depth in order to represent the typical situation where attenuation losses decrease as porosity decreases with compaction and depth. We also purposely use a Q-model that is not linearly related to the true P-wave velocity model. A grid spacing of 10 m is used to ensure there is no dispersion of P-waves; acoustic and visco-acoustic data are generated using a source wavelet with useful frequencies between 2 Hz and 18 Hz and a line of 99 sources at 6-m depth and deployed every 160 m. A total of 791 receivers at 10-m depth and a receiver spacing of 20 m are used to record pressure data.

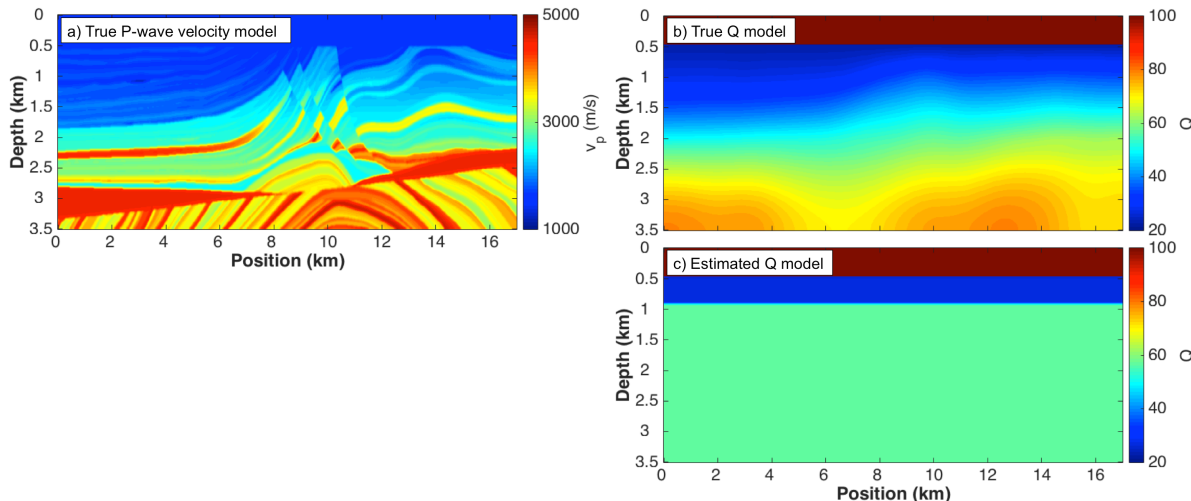


Figure 2 True a) P-wave and b) Q models for the Marmousi2 dataset, and c) estimated 1D Q model used in Step 2, obtained by taking the mean value of the true model shown in b).

Figure 3a and 3b show the acoustic and visco-acoustic pressure data generated for the models shown in Figure 2 for a representative shot gather at the centre of the model. Attenuation leads to a significant decrease in the amplitude of the events and a subtle time delay – compare Figure 3b with Figure 3a where the latter effect is visible, for example, on the first and second reflections. The difference between the two shot gathers is shown in Figure 3f.

Figure 4 shows the starting and recovered velocity models for a variety of different cases. To assess the quality of the recovered velocity model, the average relative error with respect to the true model inside the dotted area in the panels in Figure 4 is shown on the top right corner of each model. In order to simulate a more realistic situation, two independent codes are used to generate and invert the data. Figure 4a shows the original starting model, obtained by smoothing the true P-wave velocity model in Figure 2a. Figures 4b and 4c show the recovered P-wave velocity models after acoustic inversion of acoustic and visco-acoustic data, respectively. Whereas acoustic FWI of acoustic data provides an accurate recovered P-wave velocity model, the recovered model after acoustic FWI of visco-acoustic data results in a model that is less well resolved and that has lower velocities due to the phase delay and amplitude decrease introduced by attenuation.

The recovered model in Figure 4c and the average Q model in Figure 2c are now used in Step 2 of the workflow to generate acoustic and visco-acoustic data. We then proceed with Step 3 in the workflow and we obtain matching filters that match the latter to the former data, which are then applied on the observed visco-acoustic data. The resulting matched dataset (output from step 4) is inverted using a starting model obtained by smoothing the recovered model in Figure 4c in Steps 5 and 6 of the workflow. To further mitigate viscous effects, we repeat the workflow once more by performing Steps 2 to 6 again. Figure 3c shows the resulting matched dataset, whereas Figure 3g shows the difference with the acoustic data. We note some of the viscous effects have been mitigated and the amplitude and phase of the events has been changed to better match those of the acoustic data in Figure 3a.

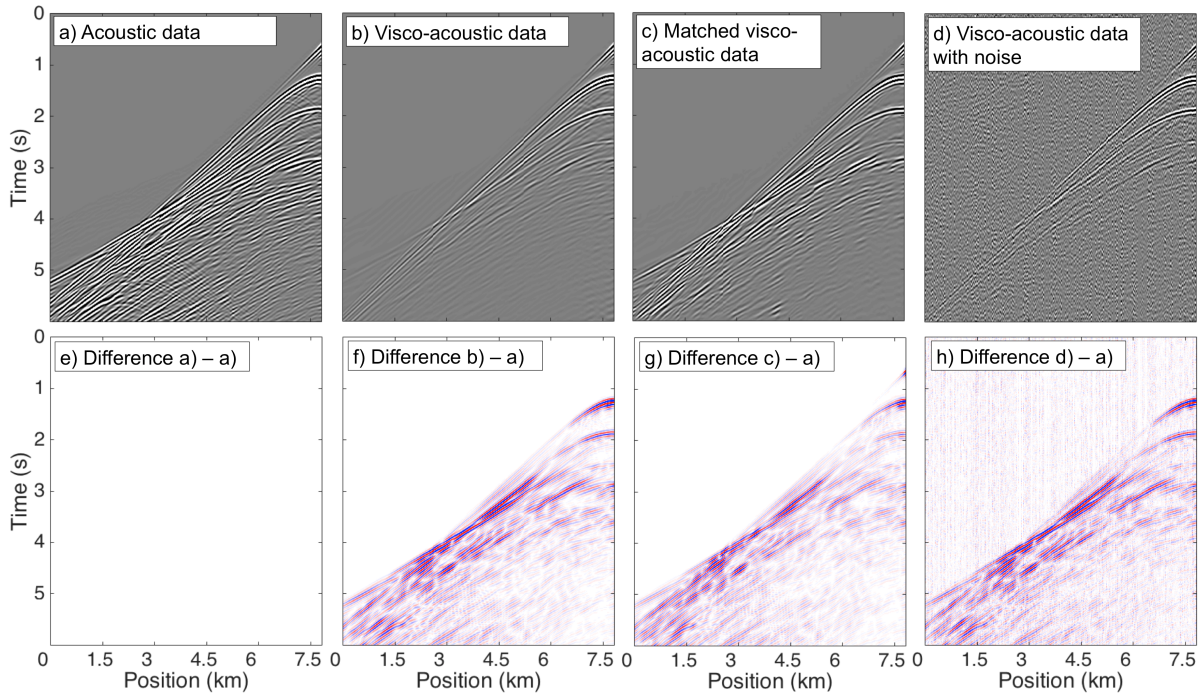


Figure 3 Top:, representative shot gather at the centre of the Marmousi2 model of a) the acoustic data, b) the visco-acoustic data, c) the matched visco-acoustic data after applying twice the suggested workflow to mitigate visco-acoustic effects, and d) the visco-acoustic data in b) with added random noise. Bottom: the difference of each of the panels above with the acoustic data in a).

Figure 4d shows the result of acoustically inverting the matched dataset. We note there is an increase in terms of resolution and also in the velocities of some of the layers, such that the recovered model is closer to the true model (note the decrease in the average relative error). The current method has been successful even though the estimated Q model is an average of the true Q model, which suggests an approximate and smooth estimated Q model is enough to mitigate the majority of the viscous effects.

Random noise was also added to the visco-acoustic data, as exemplified by the representative shot gather in Figure 3d and its difference with the acoustic data shown in Figure 3h. The noisy visco-acoustic data is then acoustically inverted resulting into the recovered model in Figure 4e. This leads to a less resolved model than that obtained after acoustic FWI of visco-acoustic data in Figure 4c, such that some of the layers at the centre of the model are no longer visible. This model and the estimated Q model in Figure 2c are then used to mitigate visco-acoustic effects using the proposed workflow in the same fashion as for the noise-free visco-acoustic data, i.e. the workflow is applied twice. Figure 4f shows the resulting recovered model, in which the resolution and velocity of the layers most affected by attenuation have clearly increased, leading to a better result than that in Figure 4e but not as good as that obtained for the noise-free data in Figure 4d due to the impact of the noise on the matching filters. Thus, the proposed workflow successfully improves the recovered P-wave velocity models by mitigating viscous effects, even in the presence of (random) noise.

Discussion

Based on the results shown for the synthetic example, application of the current method to field data requires the estimation of a not-very-accurate and smooth Q model. Methods such as that suggested by Wang (2004), based on Gabor transforms, can be efficiently used for this purpose. Furthermore, the current workflow can be combined with that presented in Agudo et al. (2016) to efficiently address visco-elastic effects in acoustic FWI without the need to use the visco-elastic equation during the inversion, thus reducing the computation costs and leading to better resolved and more accurate recovered P-wave velocity models. Note that attenuation normally produces much larger data differences than do elastic effects in FWI so that elastic FWI should always include attenuation.

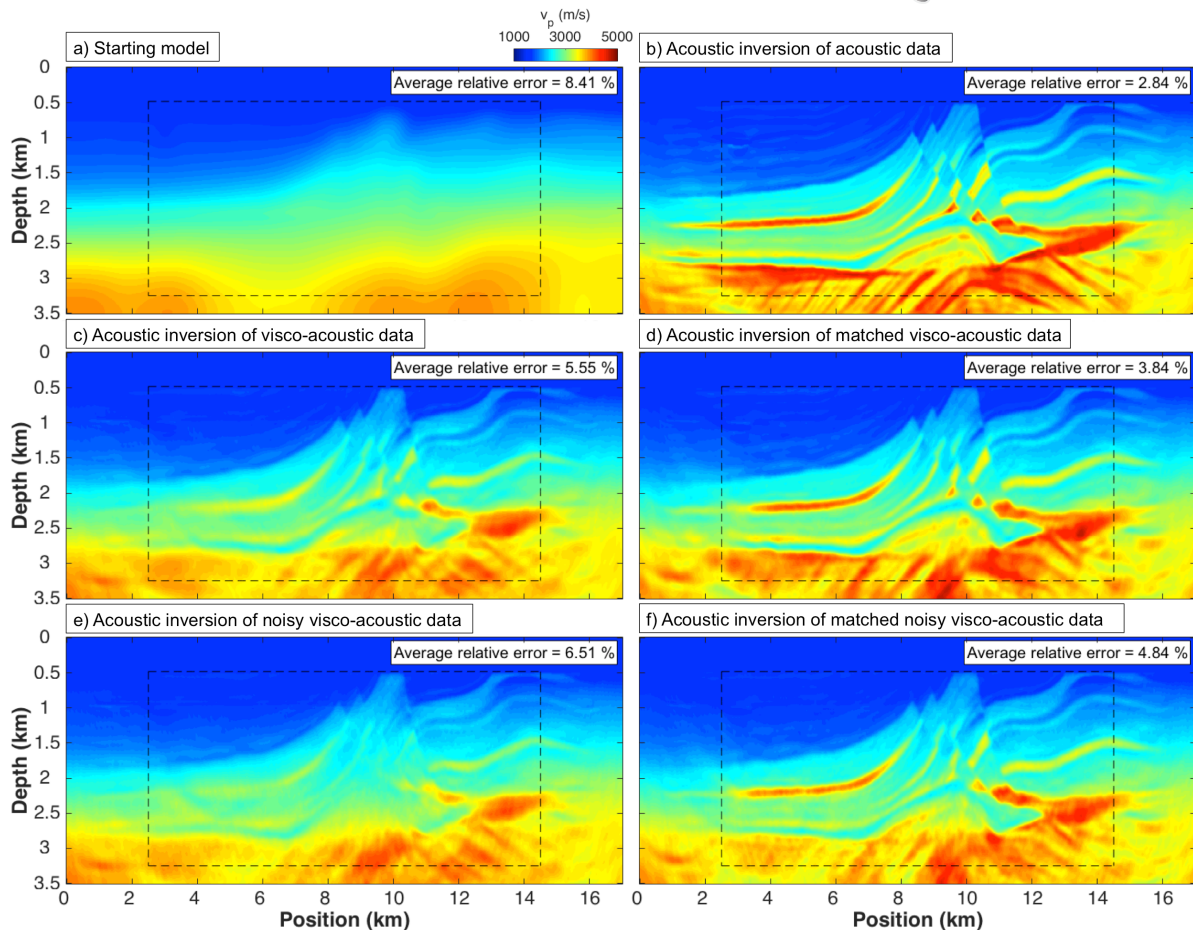


Figure 4 Vertical slices of the P-wave velocity a) starting model and the recovered models after acoustic FWI of b) acoustic data, c) visco-acoustic data, d) matched visco-acoustic data, e) visco-acoustic data with noise and f) matched visco-acoustic data with noise.

Conclusions

We have presented a workflow to mitigate viscous effects in acoustic FWI based on matching filters. Its application to the Marmousi2 synthetic model shows an improvement in the recovered P-wave velocity model in terms of resolution and accuracy of the velocities of the layers when compared to the results of acoustically inverting visco-acoustic data. An accurate attenuation model is not required and the proposed workflow is successful when applied to noisy data. The current method has also the potential to address visco-elastic effects in acoustic FWI without using a visco-elastic equation during the inversion, thus reducing the computation costs significantly.

References

- Agudo, O. C., da Silva, N. V., Warner, M. and J. Morgan, 2016, Acoustic full-waveform inversion in an elastic world: SEG Technical Program Expanded Abstracts, 1058-1062.
- Kamei, R and R. G. Pratt, 2013, Inversion strategies for visco-acoustic waveform inversion: Geophysical Journal International, **194**, 859-884.
- Stopin, A., Plessix, R. E., Kuehl, H., Goh, V. and K. Overgaag, 2016, Application of visco-acoustic FWI for gas cloud imaging and velocity model building: 78th EAGE Conference and Exhibition.
- Wang, Y., 2004, Q analysis on reflection seismic data: Geophysical Research Letters, **31**, 1-4.
- Warner, M., Morgan, J., Umpleby, A., Stekl, I., and L. Guasch, 2012, Which physics for full-wavefield seismic inversion?: 74th EAGE Conference, Extended Abstracts, 4-7.